

Original article

DOI: <https://doi.org/10.18721/JPM.16311>

## COMPUTATION OF FRACTURE PARAMETERS FOR CRACKS IN MATERIALS WITH CUBIC SYMMETRY IN THE PLANE STRAIN STATE

*A. V. Savikovskii<sup>1,2✉</sup>, A. S. Semenov<sup>1</sup>*

<sup>1</sup> Peter the Great St. Petersburg Polytechnic University, St. Petersburg, Russia;

<sup>2</sup> Joint Stock Company "Power machines – ZTL, LMZ, Electrosila,  
Energomachexport" (JSC "Power machines"), St. Petersburg, Russia;

✉ [savikovskii.artem@yandex.ru](mailto:savikovskii.artem@yandex.ru)

**Abstract.** In the paper, an oblique rectilinear central crack opening in an uniaxially tensile plane with a mixed mode of fracture (combination of normal separation and longitudinal shear modes) in two types of anisotropic materials (orthotropic one and one with cubic symmetry) has been studied. Stress intensity coefficient values for different crack orientations were calculated using expressions derived from the Lekhnitskii formalism and extrapolated methods for displacements and stresses. The results of verification of the used approach based on comparison of the finite element calculation with analytical one were presented (the difference was less than 0.75 %). A comparative analysis of the stress intensity and crack opening coefficients for three types of symmetry of elastic properties: isotropic material, material with cubic symmetry and orthotropic material was carried out.

**Keywords:** linear fracture mechanics, anisotropic material, Lekhnitskii formalism, stress intensity factor

**Funding:** The reported study was supported by The Government of the Russian Federation (State Assignment No. 0784-2020-0021).

**Citation:** Savikovskii A. V., Semenov A. S., Computation of fracture parameters for cracks in orthotropic materials and materials with cubic symmetry in the plane strain state, St. Petersburg State Polytechnical University Journal. Physics and Mathematics. 16 (3) (2023) 131–149. DOI: <https://doi.org/10.18721/JPM.16311>

This is an open access article under the CC BY-NC 4.0 license (<https://creativecommons.org/licenses/by-nc/4.0/>)

Научная статья  
УДК 539.3, 539.42  
DOI: <https://doi.org/10.18721/JPM.16311>

## РАСЧЕТ ПАРАМЕТРОВ РАЗРУШЕНИЯ ДЛЯ ТРЕЩИН В МАТЕРИАЛАХ С КУБИЧЕСКОЙ СИММЕТРИЕЙ ПРИ ПЛОСКОМ ДЕФОРМИРОВАННОМ СОСТОЯНИИ

*А. В. Савиковский<sup>1,2</sup>✉, А. С. Семенов<sup>1</sup>*

<sup>1</sup> Санкт-Петербургский политехнический университет Петра Великого, Санкт-Петербург, Россия;

<sup>2</sup> АО «Силовые машины», Санкт-Петербург, Россия

✉ [savikovskii.artem@yandex.ru](mailto:savikovskii.artem@yandex.ru)

**Аннотация.** Рассматривается наклонная прямолинейная центральная трещина в одноосно растягиваемой плоскости при смешанной моде разрушения (комбинация мод нормального отрыва и продольного сдвига) в ортотропном материале и материале с кубической симметрией. С помощью выражений, выведенных на основе формализма Лехницкого, а также методов экстраполяции перемещений и напряжений получены значения коэффициентов интенсивности напряжений для различных ориентаций трещины. Представлены результаты верификации использованного подхода на основе сравнения конечно-элементного расчета с аналитическим (отличие менее 0,75 %). Проведен сравнительный анализ коэффициентов интенсивности напряжений и раскрытия трещины для трех видов симметрии упругих свойств: изотропного материала, материала с кубической симметрией и ортотропного материала.

**Ключевые слова:** линейная механика разрушения, анизотропный материал, формализм Лехницкого, коэффициент интенсивности напряжений.

**Финансирование:** Работа выполнена при финансовой поддержке Правительства Российской Федерации (госзадание № 0784-2020-0021).

**Ссылка для цитирования:** Савиковский А. В., Семенов А. С. Расчет параметров разрушения для трещин в материалах с кубической симметрией при плоском деформированном состоянии // Научно-технические ведомости СПбГПУ. Физико-математические науки. 2023. Т. 16. № 3. С. 131–149. DOI: <https://doi.org/10.18721/JPM.16311>

Статья открытого доступа, распространяемая по лицензии CC BY-NC 4.0 (<https://creativecommons.org/licenses/by-nc/4.0/>)

### Introduction

Rotary and stationary blades of modern gas turbine engines (GTE) are their most loaded and critical elements; the loads they experience are the most diverse [1, 2]. These are centrifugal forces from rotation as well as non-uniform distribution of gas pressure and inhomogeneous temperature fields varying over time. First-stage hot section GTE blades are commonly made of single-crystal heat-resistant nickel alloys with high short-term and long-term strength, as well as high thermal fatigue resistance [3–5]. Nickel-based monocrystalline alloys are a family of orthotropic materials with cubic symmetry of elastic properties.

Diverse types of cracks can evolve in GTE blades during operation: fatigue, creep and thermal fatigue due to combined action of different loads (mentioned above), variable in time and space [6–8].

The phenomena of crack initiation and propagation under cyclic thermal loading in single crystal Ni-based alloys have been investigated experimentally, for example, in dumbbell-shaped specimens at the I.I. Polzunov Scientific and Development Association on Research and Design of Power Equipment (St. Petersburg) [5]. Finite element simulation of thermal fatigue crack nucleation in a dumbbell specimen was carried out in [9], using methods of continuum damage mechanics.



Stress intensity factors (SIF) are considered as the main fracture parameters in this study, serving to estimate the crack resistance of a structure [10, 11]. In the general cases dealing with geometry and loading for cracks in structures made of orthotropic materials, SIFs must be calculated for mixed-mode fracture (a combination of opening mode fracture, transverse and longitudinal shear). Sih, Paris and Irwin [12] obtained asymptotic expressions for displacements in a small neighborhood of the crack tip for homogeneous anisotropic material under mixed-mode loading. Ranjan and Arakere [13] provide formulas for calculating SIFs for an anisotropic material based on asymptotic expressions. Cho and Lee [14] present asymptotic expressions for displacements in the vicinity of the crack tip, formulating equations for calculating the SIFs by extrapolation of displacements for composite anisotropic material. The interaction of several cracks in an infinite anisotropic plane are considered in [15–17], accompanied by SIF calculations. Different fracture criteria based on calculating the SIFs (maximum circumferential stress, energy criterion, etc.) were proposed in various studies on fracture mechanics in isotropic materials, for example, in [18–20]. The influence from the orientation of the material's anisotropy axes on the values of SIF in an anisotropic plate was considered in [21–23]. Curvilinear cracks in an anisotropic elastic material were discussed in [24–26], exploring the specifics of SIF calculations for this type of cracks. A numerical method was used in [27, 28] to calculate SIFs for two- and three-dimensional cases, finding numerically complex roots used in asymptotic expansions for displacements.

Notably, all of the above papers calculate SIFs by the finite element method, based on asymptotic expansion of displacements or stresses in an anisotropic material [12]. However, complex parameters of an anisotropic material depending on its elastic constants have to be additionally found within this approach, with a fourth-order equation subsequently solved [12, 29].

In this paper, we propose explicit formulas for calculating SIFs in terms of orthotropic elastic constants, crack tip displacements and crack rotation angle relative to the anisotropy axes of the material (similar to the known formulas for isotropic material). This allows to calculate the SIFs in finite element (FE) computations, when only the displacements in the vicinity of the crack tip and the elastic moduli of the orthotropic material are known; these formulas are useful for engineering calculations, yielding estimates for crack resistance of structures.

Especially the proposed improvements are useful for finite element packages where the built-in methods do not allow to calculate SIFs by extrapolation of displacements for anisotropic materials (for example, ANSYS). Formulas for calculating the SIFs in terms of displacements of the crack edges and the elastic properties of the orthotropic material were obtained in [30] for the case of a plane stress state. This study proposes a generalization of the methods constructed in [30] for the case of a plane strain state.

The goal of this study is to obtain the expressions containing explicit dependences of the SIFs on the displacements of the edges in the vicinity of the crack tip in orthotropic material and material with cubic symmetry for the case of a plane strain state (PSS).

The proposed analytical expressions can be used to obtain numerical estimates for orthotropic materials based on the displacement extrapolation method. The paper also presents SIF calculations using the stress extrapolation method, comparing the results with the data obtained for the displacement extrapolation method.

The Lekhnitskii formalism is used to calculate SIFs by extrapolation of displacements and stresses [31]. The proposed relations for the displacement extrapolation method as well as formulas for the stress extrapolation method are tested for the cases of materials with different symmetry of elastic properties: isotropic, orthotropic, as well as for a material with cubic symmetry.

### Governing equations for a linear elastic material

The stress-strain state of cracked elastic bodies and the corresponding values of the fracture parameters are generally sensitive to the type of material symmetry and the elastic constants. Let us therefore consider the structure of compliance matrices for different classes of materials in this section.

The generalized Hooke's law for anisotropic material is written as follows in matrix form [32, 33]:

$$\varepsilon_i = S_{ij} \sigma_j, \quad \sigma_i = C_{ij} \varepsilon_j. \quad (1)$$

Einstein's summation convention is used in Eq. (1) and the following notations are introduced for tensor components:  $\varepsilon_i$  is a component of a 6-dimensional vector composed of strain tensor components:

$$\{\boldsymbol{\varepsilon}\} = \{\varepsilon_{xx} \quad \varepsilon_{yy} \quad \varepsilon_{zz} \quad \gamma_{yz} \quad \gamma_{xz} \quad \gamma_{xy}\}^T;$$

$\sigma_j$  is a component of a 6-dimensional stress vector

$$\{\boldsymbol{\sigma}\} = \{\sigma_{xx} \quad \sigma_{yy} \quad \sigma_{zz} \quad \sigma_{yz} \quad \sigma_{xz} \quad \sigma_{xy}\}^T;$$

$S_{ij}$  is an element of the compliance matrix ( $6 \times 6$ );  $C_{ij}$  is an element of the elastic modulus matrix ( $6 \times 6$ ).

The  $3 \times 3$  compliance matrix for the case of a plane strain state has a different form (depending on the symmetry class).

For orthotropic material

$$[\mathbf{S}]_{PDS} = \begin{bmatrix} S_{11}^{PDS} & S_{12}^{PDS} & S_{16}^{PDS} \\ S_{21}^{PDS} & S_{22}^{PDS} & S_{26}^{PDS} \\ S_{16}^{PDS} & S_{26}^{PDS} & S_{66}^{PDS} \end{bmatrix} = \begin{bmatrix} \frac{1-\nu_{13}\nu_{31}}{E_1} & -\frac{\nu_{12}}{E_1} - \frac{\nu_{13}\nu_{32}}{E_1} & 0 \\ -\frac{\nu_{12}}{E_1} - \frac{\nu_{13}\nu_{32}}{E_1} & \frac{1-\nu_{23}\nu_{32}}{E_2} & 0 \\ 0 & 0 & \frac{1}{G_{12}} \end{bmatrix}; \quad (2)$$

for material with cubic symmetry:

$$[\mathbf{S}]_{PDS} = \begin{bmatrix} S_{11}^{PDS} & S_{12}^{PDS} & S_{16}^{PDS} \\ S_{21}^{PDS} & S_{22}^{PDS} & S_{26}^{PDS} \\ S_{16}^{PDS} & S_{26}^{PDS} & S_{66}^{PDS} \end{bmatrix} = \begin{bmatrix} \frac{1-\nu^2}{E} & -\frac{\nu(\nu+1)}{E} & 0 \\ -\frac{\nu(\nu+1)}{E} & \frac{1-\nu^2}{E} & 0 \\ 0 & 0 & \frac{1}{G} \end{bmatrix}; \quad (3)$$

For isotropic material

$$[\mathbf{S}]_{PDS} = \begin{bmatrix} S_{11}^{PDS} & S_{12}^{PDS} & S_{16}^{PDS} \\ S_{21}^{PDS} & S_{22}^{PDS} & S_{26}^{PDS} \\ S_{16}^{PDS} & S_{26}^{PDS} & S_{66}^{PDS} \end{bmatrix} = \begin{bmatrix} \frac{1-\nu^2}{E} & -\frac{\nu(\nu+1)}{E} & 0 \\ -\frac{\nu(\nu+1)}{E} & \frac{1-\nu^2}{E} & 0 \\ 0 & 0 & \frac{2(\nu+1)}{E} \end{bmatrix}, \quad (4)$$

where  $E_1, E_2, E_3$  are Young's moduli;  $G_{23}, G_{13}, G_{12}, G$  are the shear moduli;  $\nu_{31}, \nu_{13}, \nu_{23}, \nu_{32}, \nu_{12}, \nu$  are Poisson's ratios.

### Methods for calculating SIFs

We consider a problem of uniaxial tension along the vertical direction in an orthotropic plate (plane) with a single oblique rectilinear central crack assuming a plane strain state. It is assumed that the normal to the plate coincides with one of the orthotropy axes. The axes of the introduced global Cartesian coordinate system  $xOy$  coincide with the anisotropy axes of the material  $x \gg Oy \gg$  and the loading direction  $Ox$ . The crack orientation  $Ox'$  does not coincide with the anisotropy axes  $x''Oy''$  of the material and the loading direction  $Ox$  (Fig. 1).

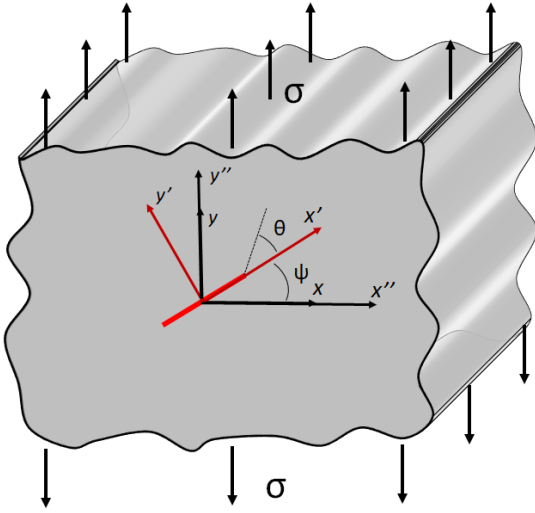


Fig. 1. Schematic representation of problem statement: orthotropic plate (finite or infinite) with an oblique rectilinear crack (highlighted by a red line) with a plane strain state (PSS) under the action of uniaxial tension:

3 coordinate systems are shown,  $\psi$  is the crack inclination angle relative to the global coordinate system,  $\theta$  is the angle between the direction to the analyzed point and the crack coordinate system

Asymptotic expressions for displacements near the crack in a polar coordinate system with the origin at the crack tip are well known for an isotropic material for the case of PSS [34]; these expressions are used to calculate the SIFs by displacement extrapolation [35]:

$$\begin{aligned} K_I &= \sqrt{\frac{2\pi}{r}} \cdot \frac{G}{2(1-\nu)} \cdot u'_y(r, \pi), \\ K_{II} &= \sqrt{\frac{2\pi}{r}} \cdot \frac{G}{2(1-\nu)} \cdot u'_x(r, \pi), \end{aligned} \quad (5)$$

where  $G = \frac{E}{2(1+\nu)}$  and  $\nu$  are the shear modulus

and Poisson's ratio of the isotropic material;  $r$  is the distance from the crack tip to the point under consideration;  $K_I$ ,  $K_{II}$  are the SIF values for the opening-mode fracture and longitudinal shear;  $u'_x(r, \pi)$ ,  $u'_y(r, \pi)$  are the components of the displacement vector of the upper edge of the crack in the crack coordinate system.

The expressions for SIFs in the case of anisotropic material, similar to (5), are obtained from the asymptotic expressions for displacement fields at the crack tip assuming that  $x_3 = z = 0$ ,

and the presence of a PSS. The expressions derived based on the Lekhnitskii formalism [31] allow for the following representation [13]:

$$\begin{aligned} u'_x(r, \theta) &= \sqrt{\frac{2r}{\pi}} \cdot \operatorname{Re} \left( \frac{1}{\mu'_1 - \mu'_2} \cdot \sum_{i=1}^2 \sum_{j=1}^2 (K_i M_{ij} p_j \sqrt{\cos \theta + \mu'_j \sin \theta}) \right), \\ u'_y(r, \theta) &= \sqrt{\frac{2r}{\pi}} \cdot \operatorname{Re} \left( \frac{1}{\mu'_1 - \mu'_2} \cdot \sum_{i=1}^2 \sum_{j=1}^2 (K_i M_{ij} q_j \sqrt{\cos \theta + \mu'_j \sin \theta}) \right), \end{aligned} \quad (6)$$

where  $u'_x(r, \theta)$ ,  $u'_y(r, \theta)$  are the components of the displacement vector in the polar coordinate system of the crack;  $r$  is the distance from the crack tip to the point under consideration;  $\theta$  is the angle between the direction to the analyzed point and the direction of crack growth;  $K_1$ ,  $K_2$  are the

SIF values corresponding to modes I and II, respectively ( $K_I = K_1$ ,  $K_{II} = K_2$ );  $M_{ij} = \begin{bmatrix} -\mu'_2 & \mu'_1 \\ -1 & 1 \end{bmatrix}$  is the auxiliary matrix.

Eq. (6) can be reduced by identical algebraic transformations to the form used in [13, 30, 36]. The quantities  $p_i$  and  $q_i$  depend on  $\mu_i$  according to the corresponding formulas [13, 30];  $\mu'_1$ ,  $\mu'_2$  are complex parameters of the anisotropic material, i.e., the roots of the 4th-order equation with compliance constants in the crack coordinate system [31], selected so that the roots have a positive imaginary part.

It should be noted that expressions (6) are valid for orthotropic material and cubic symmetry in a plane stress or plane strain state; however, expressions (6) become more complicated for a crack in a three-dimensional stress state (see [37]).

Substituting the value  $\theta = \pi$  into expressions (6) and converting them, we obtain the required values of SIFs for the case of an anisotropic material [25, 36]:

$$\{\mathbf{K}\} = \sqrt{\frac{\pi}{2r}} \cdot [\mathbf{B}]^{-1} \cdot \{\mathbf{u}'\}, \quad (7)$$

where  $\{\mathbf{K}\} = \{K_I, K_{II}\}^T$ ,  $\{\mathbf{u}'\} = \{u'_x(r, \pi), u'_y(r, \pi)\}^T$ .

$$[\mathbf{B}]^{-1} = \begin{bmatrix} \frac{1}{\det[\mathbf{B}]} \operatorname{Re} \left( \frac{\mu'_1 p_2 - \mu'_2 p_1}{\mu'_1 - \mu'_2} i \right) & \frac{1}{\det[\mathbf{B}]} \operatorname{Re} \left( -\frac{p_2 - p_1}{\mu'_1 - \mu'_2} i \right) \\ \frac{1}{\det[\mathbf{B}]} \operatorname{Re} \left( -\frac{\mu'_1 q_2 - \mu'_2 q_1}{\mu'_1 - \mu'_2} i \right) & \frac{1}{\det[\mathbf{B}]} \operatorname{Re} \left( \frac{q_2 - q_1}{\mu'_1 - \mu'_2} i \right) \end{bmatrix}. \quad (8)$$

The primes on the quantities in the ratios (5)–(8) indicate that these components of vectors and tensors belong to the coordinate system associated with the crack orientation ( $x'Oy'$  in Fig. 1).

If the  $xOy$  coordinate system is rotated into the  $x'Oy'$  coordinate system in the plane by an angle  $\psi$  (see Fig. 1), the matrix is determined by the equality

$$[\mathbf{Q}] = \begin{bmatrix} \cos \psi & \sin \psi & 0 \\ -\sin \psi & \cos \psi & 0 \\ 0 & 0 & 1 \end{bmatrix} \quad (9)$$

and the elastic compliance matrix is transformed from the global coordinate system to the crack coordinate system via the transformation matrix, based on the ratio

$$S'_{ijkl} = Q_{im} \cdot Q_{jn} \cdot Q_{ko} \cdot Q_{lp} \cdot S_{mnop}, \quad (9)$$

in turn transformed into the Lekhnitskii formulas in the two-dimensional case [31].

Interestingly, the components of the displacement vector in expressions (5) and (8) must also be given in the coordinate system associated with the crack:

$$u'_i = Q_{im} u_m. \quad (10)$$

Thus, expressions (7) and (8) can be used to calculate the SIF values if the displacements in the crack edges and the linear elastic constants of the material are known.

The SIFs can also be determined from the asymptotic expressions (see [13, 32, 38] for PSS) for the distribution of stress fields along the crack growth direction ( $\theta = 0$ ):

$$u'_i = Q_{im} u_m. \quad (10)$$

$$\begin{aligned} K_I &= \sigma'_{yy}(r, 0) \cdot \sqrt{2\pi r}, \\ K_{II} &= \sigma'_{xx}(r, 0) \cdot \sqrt{2\pi r}, \end{aligned} \quad (11)$$

We should note that expressions (11) are valid for both isotropic and anisotropic materials.

If relations (11) are used, the stress components also need to be transformed from the global coordinate system  $xOy$  to the crack coordinate system  $x'Oy'$  (see Fig. 1):

$$\sigma'_{ij} = Q_{im} Q_{jn} \sigma_{mn}. \quad (12)$$

### Formulating the SIF expressions for specific classes of elastic symmetry properties

According to Eqs. (6)–(8), the complex parameters of anisotropic material  $\mu'_1$  and  $\mu'_2$  need to be found to calculate SIFs in terms of the components of the displacement vector, based on the 4th-order characteristic equation. In the case when the crack is not rotated relative to the anisotropy axes of the material, the characteristic equation for determining  $\mu_1$  and  $\mu_2$  takes the form:

$$S_{11}\mu^4 - 2S_{16}\mu^3 + (2S_{12} + S_{66})\mu^2 - 2S_{26}\mu + S_{22} = 0 \quad (13)$$

Substituting the coefficients  $S_{ij}$  for the orthotropic material for the case of PSS (2) into Eq. (13), we solve it using the formulas for converting the roots to the crack coordinate system; then, substituting the calculated roots  $\mu_1$  and  $\mu_2$  into expressions for  $[\mathbf{B}]^{-1}$  (8), we arrive at an explicit analytical expression for the influence matrix  $[\mathbf{B}]^{-1}$  in terms of the elastic moduli of orthotropic material:

$$[\mathbf{B}]^{-1} = \begin{bmatrix} C \left( 1 - \sqrt{\frac{E_1(1-v_{23}v_{32})}{E_2(1-v_{13}v_{31})}} \right) \sin 2\psi & 2C \left( \sqrt{\frac{E_1(1-v_{23}v_{32})}{E_2(1-v_{13}v_{31})}} \sin^2 \psi + \cos^2 \psi \right) \\ 2C \left( \sqrt{\frac{E_1(1-v_{23}v_{32})}{E_2(1-v_{13}v_{31})}} \cos^2 \psi + \sin^2 \psi \right) & C \left( 1 - \sqrt{\frac{E_1(1-v_{23}v_{32})}{E_2(1-v_{13}v_{31})}} \right) \sin 2\psi \end{bmatrix}, \quad (14)$$

where  $C = \frac{1}{2} \sqrt{\frac{E_1 E_2}{\left( 2 \sqrt{\frac{E_1}{E_2}} \sqrt{(1-v_{13}v_{31})(1-v_{23}v_{32})} + \left( \frac{E_1}{G_{12}} - 2(v_{12} + v_{13}v_{32}) \right) \right) (1-v_{23}v_{32})}}$ .

As a corollary to Eq. (7), the SIFs for an orthotropic material are determined in terms of the components of the displacement vector in the small neighborhood of the crack tip with a PSS based on the relations:

$$\begin{aligned} K_I &= \sqrt{\frac{\pi}{2r}} \left( C \left( 1 - \sqrt{\frac{E_1(1-v_{23}v_{32})}{E_2(1-v_{13}v_{31})}} \right) \sin 2\psi \cdot u'_x + 2C \left( \sqrt{\frac{E_1(1-v_{23}v_{32})}{E_2(1-v_{13}v_{31})}} \sin^2 \psi + \cos^2 \psi \right) \cdot u'_y \right), \\ K_{II} &= \sqrt{\frac{\pi}{2r}} \left( 2C \left( \sqrt{\frac{E_1(1-v_{23}v_{32})}{E_2(1-v_{13}v_{31})}} \cos^2 \psi + \sin^2 \psi \right) \cdot u'_x + C \left( 1 - \sqrt{\frac{E_1(1-v_{23}v_{32})}{E_2(1-v_{13}v_{31})}} \right) \sin 2\psi \cdot u'_y \right). \end{aligned} \quad (15)$$

Notably, each SIF ( $K_I$  and  $K_{II}$ ) in Eq. (15) depends on both displacement components  $u'_x$  and  $u'_y$ .

In the case of calculating SIFs for cracks in materials with cubic symmetry, expressions (15) are simplified (taking into account the equalities  $E_1 = E_2 = E$ ,  $G_{12} = G_{13} = G_{23} = G$ ;  $v_{12} = v_{13} = v_{31} = v_{23} = v_{32} = v_{21} = v$ ):

$$\begin{aligned} K_I &= \sqrt{\frac{\pi}{2r}} \cdot \frac{E}{\sqrt{(1-v^2) \left( \frac{E}{G} + 2(1-2v)(1+v) \right)}} \cdot u'_y, \\ K_{II} &= \sqrt{\frac{\pi}{2r}} \cdot \frac{E}{\sqrt{(1-v^2) \left( \frac{E}{G} + 2(1-2v)(1+v) \right)}} \cdot u'_x. \end{aligned} \quad (16)$$

The matrix  $[\mathbf{B}]^{-1}$  is diagonal in this case, i.e., each component of the displacement vector affects only one SIF and not the other. Moreover, the difference between ratios (16) and expressions (15) is that the crack inclination angles has absolutely no effect on the SIF values.

There is an important qualitative difference between Eq. (15) obtained for the case of a plane strain state and a similar formula in [30] for the case of a plane stress state. In the case of PSS, the SIFs depend on the Poisson ratios  $\nu_{13}, \nu_{23}, \nu_{31}, \nu_{32}$ .

Consider the properties of the matrix  $[\mathbf{B}]^{-1}$ .

*Property 1.* The determinant of the matrix  $[\mathbf{B}]^{-1}$  depends only on the parameter  $C$ :

$$\det [\mathbf{B}]^{-1} = 4\tilde{N}^2 \cdot \left( \left( 1 + \frac{E_1(1-\nu_{23}\nu_{32})}{E_2(1-\nu_{13}\nu_{31})} - 2\sqrt{\frac{E_1(1-\nu_{23}\nu_{32})}{E_2(1-\nu_{13}\nu_{31})}} \right) \sin^2 \psi \cos^2 \psi - \frac{E_1(1-\nu_{23}\nu_{32})}{E_2(1-\nu_{13}\nu_{31})} \sin^2 \psi \cos^2 \psi - \sin^2 \psi \cos^2 \psi - \sqrt{\frac{E_1(1-\nu_{23}\nu_{32})}{E_2(1-\nu_{13}\nu_{31})}} \cdot (\sin^4 \psi + \cos^4 \psi) \right) = -4\tilde{N}^2.$$

It follows from the expression for  $\det[\mathbf{B}]^{-1}$  that it is impossible to uniquely calculate the SIF in terms of displacements if  $C = 0$  or  $C \rightarrow \infty$ . It follows from the conditions  $E_1 > 0, E_2 > 0$  that  $C \neq 0$ , however, a possible situation is that  $C \rightarrow \infty$ , which happens provided that

$$2\sqrt{\frac{E_1}{E_2}} \sqrt{(1-\nu_{13}\nu_{31})(1-\nu_{23}\nu_{32})} + \left( \frac{E_1}{G_{12}} - 2(\nu_{12} + \nu_{13}\nu_{32}) \right) = 0,$$

$$\left( \frac{E_1}{G_{12}} - 2(\nu_{12} + \nu_{13}\nu_{32}) \right) < 0.$$

This ratio between the elastic constants corresponds to the formula for the roots of Eq. (13) when they are real, but Eq. (13) cannot have real roots [31]. If the ratio of elastic constants is sufficiently close to

$$2\sqrt{\frac{E_1}{E_2}} \sqrt{(1-\nu_{13}\nu_{31})(1-\nu_{23}\nu_{32})} + \left( \frac{E_1}{G_{12}} - 2(\nu_{12} + \nu_{13}\nu_{32}) \right) \approx 0,$$

or  $E_1$  is sufficiently small, it may prove problematic to numerically determine the matrix  $[\mathbf{B}]^{-1}$  and calculate the SIFs.

*Property 2.* As follows from expression (15), in the case when

$$E_1(1-\nu_{23}\nu_{32}) = E_2(1-\nu_{13}\nu_{31})$$

the elements of the matrix  $[\mathbf{B}]^{-1}$  do not depend on the crack rotation angle  $\psi$  (just as in the case of an isotropic material);  $u'_y$  only affects  $K_I$ ,  $u'_x$  only affects  $K_{II}$ .

*Property 3.* As evident from expressions (15), the closer the root  $\sqrt{\frac{E_1(1-\nu_{23}\nu_{32})}{E_2(1-\nu_{13}\nu_{31})}}$  is to unity, the more  $u'_y$  affects the value of  $K_I$  and  $u'_x$  the value of  $K_{II}$ , and vice versa.

### Testing the methods for calculating SIFs using the finite element solution of the problem

We consider an oblique rectilinear through crack in an infinite plate (plane) oriented at an angle  $\psi$  to the anisotropy axes (Fig. 2), with uniaxial tension of the plate in the vertical direction. It is assumed that the PSS is achieved in the problem when the stress-strain state is the same in each section along the  $z$  axis and  $\varepsilon_{xz} = \gamma_{xz} = \gamma_{yz} = 0$ . The SIFs are calculated for different crack orientations, varied in increments of  $30^\circ$ , to test the obtained formulas based on extrapolation methods for displacements and stresses. The finite element method is used to calculate SIFs in computations of stress and displacement fields [39–41]. The plate material is considered to be linearly elastic.



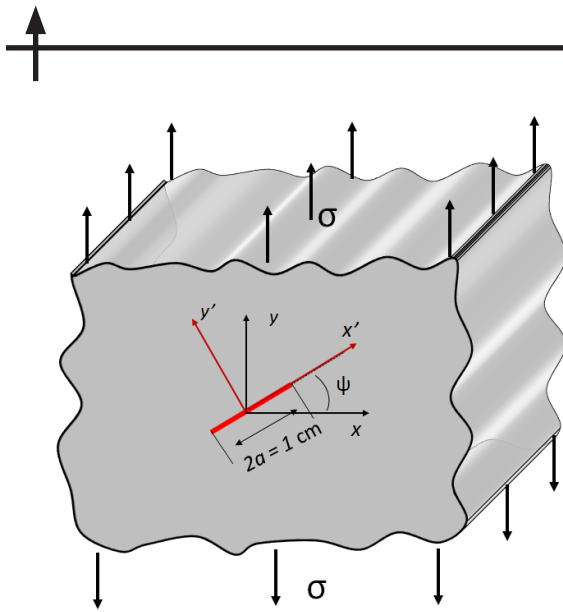


Fig. 2. Schematic representation of problem statement for uniaxial tension of an infinite plate with an oblique through crack (highlighted in red)

This problem has a well-known analytical solution for SIFs [42]:

$$K_I = \sigma\sqrt{\pi a} \cdot \cos^2 \psi, \tag{17}$$

$$K_{II} = \sigma\sqrt{\pi a} \cdot \sin \psi \cdot \cos \psi.$$

The analytical solution for the infinite plane in Eqs. (17) does not depend on the form of anisotropy and the elastic moduli of the material. This is because an infinite plane is considered and the loads are self-balanced. SIF computations for isotropic and anisotropic materials using the displacement method (see Eqs. (5), (15) and (16)) and stress method (see Eqs. (12) and (13)) were performed in the PANTOCRATOR finite element package [43]. Quadratic plane 8-node elements were used in the computations.

Several FE models of a cracked plate were constructed in the computations, varying the angle  $\psi$  (crack orientation angle relative to the orthotropy axes of of the material) and compar-

ing the numerical values of the SIFs with the analytical ones. Fig. 3 shows as an example the FE model of a square plate with a central rectilinear crack inclined at an angle  $\psi = 60^\circ$ , including 126,000 nodes, 20,800 finite elements in the entire model and 80 at the edge of the crack.

The behavior of a crack in an infinite plate (plane) was simulated for a plate of finite dimensions, a 1:22 ratio was chosen between the length of the computational domain and the crack: the length of the domain for simulation was 22 cm, the width of the domain was also 22 cm; the length of the crack was 1 cm. The load in the problem was a constant vertical stress  $\sigma_{yy} = 100$  MPa, set at the upper face. The plate was fixed to exclude solid-state displacements. Numerical methods were verified and comparing with the analytical solution for three types of elastic properties:

- isotropic material,
- material with cubic symmetry,
- orthotropic material.

The values of the elastic constants used in the calculations are taken from [30]. Fig. 4 shows a comparison of SIF values obtained by extrapolation of displacements and stresses with analytical solution (17) for all three types of material properties.

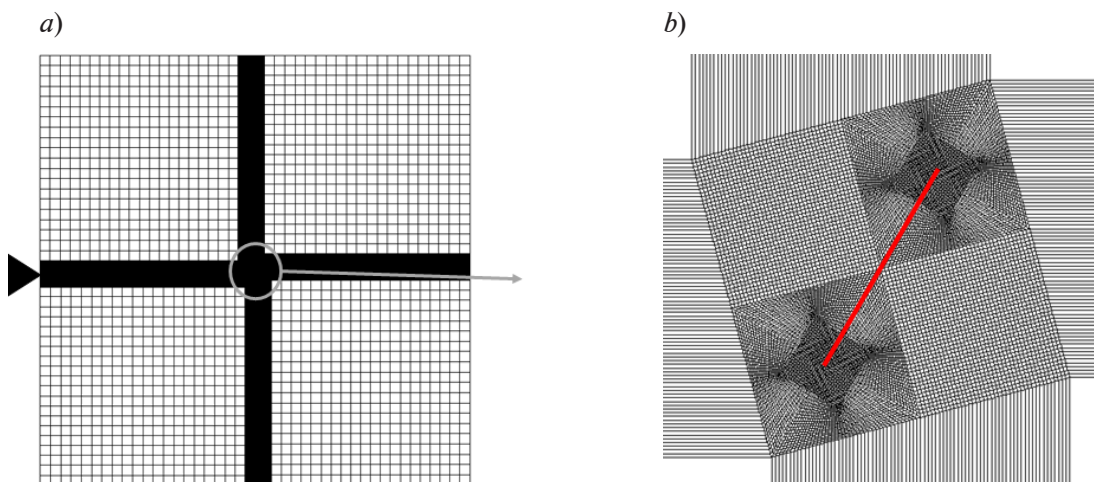


Fig. 3. FE model of plate with oblique central crack (a) and its enlarged fragment in the vicinity of the crack (b)

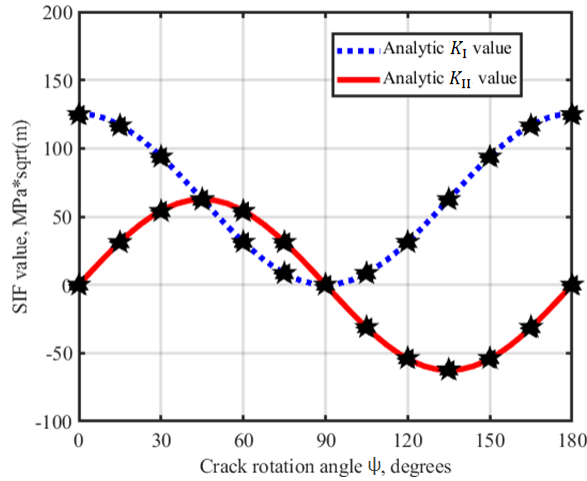


Fig. 4. Graphs comparing the values of SIFs  $K_I$  and  $K_{II}$ , obtained numerically by extrapolation of displacements (symbols), with an analytical solution for SIFs  $K_I$  (blue dashed line) and  $K_{II}$  (solid red line). Values for an isotropic material are marked with the symbol (▲), those for an orthotropic material with (◄), those for a material with cubic symmetry of properties with (◆)

Analytical and numerical values of  $K_I$  and  $K_{II}$  for inclination angles that are multiples of  $30^\circ$  (marked with symbols in Fig. 4), are given in Table 1. We should note that the maximum error  $\Delta_{\max}$  for the method calculating SIFs by the stresses (0.40%) is lower than that for the method calculating SIFs by the displacements (0.75%). Error for isotropic material is minimal, and maximal for both methods for orthotropic material. However, despite this, these methods show high accuracy, since the error does not exceed 0.75% compared with the analytical solution in all cases considered.

### Influence of material anisotropy on crack opening

We compare the opening of the crack edges for the three previously considered classes of materials: isotropic, with cubic symmetry and orthotropic. If we consider expressions (6) for SIFs of the isotropic material and transform them by subtracting the displacement at the opposite edges of the crack, then, after substituting analytical expression (17) for the SIFs, we obtain the following equalities for opening of the crack in the isotropic material:

$$u'_x(r, \pi) - u'_x(r, -\pi) = 2\sigma_0 \sqrt{2ra} \sin \psi \cdot \cos \psi \frac{2(1-\nu^2)}{E}, \quad (18)$$

$$u'_y(r, \pi) - u'_y(r, -\pi) = 2\sigma_0 \sqrt{2ra} \cos^2 \psi \frac{2(1-\nu^2)}{E}.$$

If we use the expressions from our earlier paper [30] for the displacements of the crack edges in the anisotropic material and substitute the expressions for complex roots into expressions for the matrix  $[\mathbf{B}]^{-1}$ , followed by substitution of expressions (17) for SIFs, then in the case of cubic symmetry we obtain the following expressions for crack opening:

$$u'_x(r, \pi) - u'_x(r, -\pi) = 2\sigma_0 \sqrt{2ra} \sin \psi \cdot \cos \psi \frac{\sqrt{(1-\nu^2) \cdot \left( \frac{E}{G} + 2(1-2\nu)(1+\nu) \right)}}{E}, \quad (19)$$

$$u'_y(r, \pi) - u'_y(r, -\pi) = 2\sigma_0 \sqrt{2ra} \cos^2 \psi \frac{\sqrt{(1-\nu^2) \cdot \left( \frac{E}{G} + 2(1-2\nu)(1+\nu) \right)}}{E}.$$

Similarly, we can obtain the following expressions for the orthotropic material:

$$\begin{aligned}
 u'_x(r, \pi) - u'_x(r, -\pi) &= 2\sigma_0 \sqrt{2ra} \sin \psi \cdot \cos \psi \times \\
 &\times \sqrt{\frac{(1 - \nu_{23}\nu_{32}) \cdot \left( 2\sqrt{\frac{E_1}{E_2}} \sqrt{(1 - \nu_{13}\nu_{31})(1 - \nu_{23}\nu_{32})} + \left( \frac{E_1}{G_{12}} - 2(\nu_{12} + \nu_{13}\nu_{32}) \right) \right)}{E_1 E_2}}, \\
 u'_y(r, \pi) - u'_y(r, -\pi) &= 2\sigma_0 \sqrt{2ra} \cos^2 \psi \times \\
 &\times \sqrt{\frac{(1 - \nu_{23}\nu_{32}) \cdot \left( 2\sqrt{\frac{E_1}{E_2}} \sqrt{(1 - \nu_{13}\nu_{31})(1 - \nu_{23}\nu_{32})} + \left( \frac{E_1}{G_{12}} - 2(\nu_{12} + \nu_{13}\nu_{32}) \right) \right)}{E_1 E_2}}.
 \end{aligned}
 \tag{20}$$

Table 1

**Comparison of computational results with analytical solution for three types of material**

$\psi$ , deg	SIF value, MPa·m <sup>1/2</sup>						$\Delta_{\max}$ , %	
	Analytical solution		Displacement method		Stress method		DM	SM
	$K_I$	$K_{II}$	$K_I$	$K_{II}$	$K_I$	$K_{II}$		
<i>Isotropic material</i>								
0	125.33	0.00	125.01	1·10 <sup>-4</sup>	125.31	0.001	0.25	0.01
30	93.99	54.26	93.74	53.89	93.97	54.23	0.70	0.07
60	31.33	54.26	31.24	53.88	31.31	54.21	0.72	0.11
90	0.00	0.00	1·10 <sup>-4</sup>	2·10 <sup>-4</sup>	1·10 <sup>-4</sup>	1·10 <sup>-4</sup>	0.02	0.01
120	31.33	-54.26	31.23	-53.87	31.29	31.29	0.73	0.14
150	93.99	-54.26	93.74	-53.89	93.96	93.96	0.70	0.07
180	123.33	0.00	125.01	1·10 <sup>-4</sup>	125.31	125.31	0.25	0.01
<i>Material with cubic symmetry</i>								
0	125.33	0	124.84	0.004	125.13	0.003	<b>0.39</b>	<b>0.16</b>
30	93.99	54.27	93.73	53.87	93.95	54.20	0.73	0.13
60	31.33	54.27	31.27	53.92	31.35	54.27	0.64	0.11
90	0	0	1·10 <sup>-4</sup>	2·10 <sup>-4</sup>	1·10 <sup>-4</sup>	1·10 <sup>-4</sup>	0.02	0.01
120	31.33	-54.27	31.26	-53.91	31.32	-54.20	0.66	0.13
150	93.99	-54.27	93.73	-53.87	93.95	-54.26	0.73	0.13
180	125.33	0	124.84	0.004	125.13	0.003	0.39	0.16
<i>Orthotropic material</i>								
0	125.33	0	124.54	0.006	124.82	0.007	0.63	0.40
30	93.99	54.27	93.72	54.36	93.86	54.24	0.29	0.14
60	31.33	54.27	31.43	53.99	31.42	54.29	0.66	0.28
90	0	0	1·10 <sup>-4</sup>	2·10 <sup>-4</sup>	1·10 <sup>-4</sup>	1·10 <sup>-4</sup>	0.01	0.01
120	31.33	-54.27	31.45	-53.98	31.37	-54.29	0.75	0.11
150	93.99	-54.27	93.72	-54.36	93.86	-54.24	0.29	0.14
180	125.33	0	124.54	0.006	124.82	0.0068	0.63	0.40

Notations:  $\psi$  is the crack inclination angle relative to the  $x$  axis;  $\Delta_{\max}$  is the maximum error for the SIFs  $K_I$  and  $K_{II}$ ; DM, SM are the displacement and stress methods, respectively.

The following conclusions can be drawn by comparing expressions (18)–(20):

Firstly, if  $\frac{E}{G} > 2(1 + \nu)$ , then the crack opening in the case of the material with cubic symmetry

is greater than in the case of the isotropic material with the same values of Young’s modulus  $E$  and Poisson’s ratio  $\nu$ , and vice versa.

Secondly, if we assume for convenience that Poisson’s ratios are equal for the orthotropic material and the material with cubic symmetry, i.e.,  $\nu_{12} = \nu_{23} = \nu_{31} = \nu$ , and  $E_1 = E_3 = E$  and  $G_{12} = G_{23} = G_{31} = G$ , then the crack opening for  $E_1 > E_2$  in the case of orthotropic material is greater than that for the material with cubic symmetry, and vice versa.

FE computations were performed to verify the above conclusions with different types of material symmetry and values of elastic constants. The elastic properties of all three types of material considered were set so that the crack opening was the largest for orthotropic material, the smallest for isotropic material, and intermediate for material with cubic symmetry (Table 2). The properties of the materials were selected so that the compliance matrices and elastic moduli meet the conditions of positive definiteness (see Table 2).

Fig. 5 shows the differences in the crack opening as well as in the distribution of vertical stress fields  $\sigma_y$  for different types of material anisotropy for the case of the crack angle  $\psi = 30^\circ$ . The results of FE computations qualitatively and quantitatively confirm the analytical conclusions. The latter are the same for any crack rotation angle  $\psi$ .

In practice, the anisotropy of properties in the case of materials with cubic symmetry is evaluated using the parameter

$$p = \frac{E}{G} - 2\nu, \tag{21}$$

where  $E$  is Young’s modulus,  $G$  is the shear modulus,  $\nu$  is Poisson’s ratio.

For an isotropic material,  $p = 2$ . It is preferable to isolate this parameter in Eq. (19) and plot the dependence of the opening near the crack tip (Fig. 6) from the asymptotic formulas (for example, at a given fixed distance from the tip  $r = a/20$ ). Fig. 6 also shows a dependence of the maximum crack opening ( $r = a$ ) for cubic symmetry, obtained based on the FE solution. The selected values of Young’s modulus and Poisson’s ratio are given in Table 2, the shear modulus  $G$  was varied in the range of 1–19 GPa. The external tensile load and the crack length correspond to the formulation of the problem shown in Fig. 3. The crack inclination angle  $\psi = 30^\circ$ .

As can be seen from Fig. 6, an increase in the crack opening is observed with an increase in the anisotropy parameter  $p$ . In accordance with expression (19), the dependence of crack opening on  $p$  (for fixed values of  $E$ ,  $\nu$  and a variable value of  $G$ ) has a root dependence.

Table 2

**Elastic properties for three types of material, used in FE calculations to verify crack openings**

Material	Module, GPa		Poisson’s ratio
	Young’s	shear	
Isotropic	$E = 20$	$G = 7.69$	$\nu = 0.3$
With cubic symmetry	$E = 20$	$G = 1.00$	$\nu = 0.3$
Orthotropic	$E_1 = 20$	$G_{12} = 1.00$	$\nu_{12} = 0.3$
	$E_2 = 4$	$G_{23} = 1.00$	$\nu_{23} = 0.3$
	$E_3 = 20$	$G_{31} = 1.00$	$\nu_{31} = 0.3$

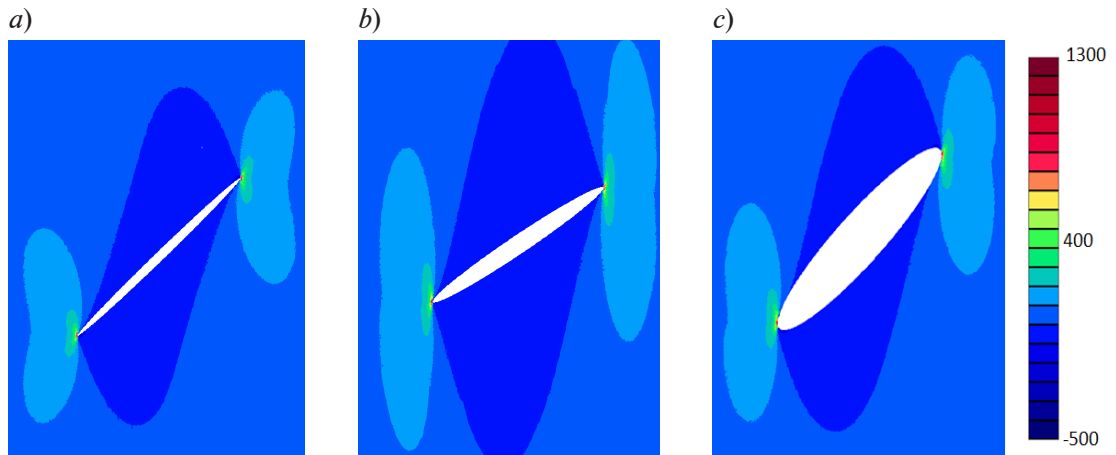


Fig. 5. Distribution of vertical stress fields  $\sigma_{yy}$  [MPa] (initial inclination angle  $\psi = 30^\circ$ ) for materials with different symmetry of elastic properties: isotropic (a), cubic (b) and orthotropic (c). The scale of displacements is magnified by 5 times for clarity

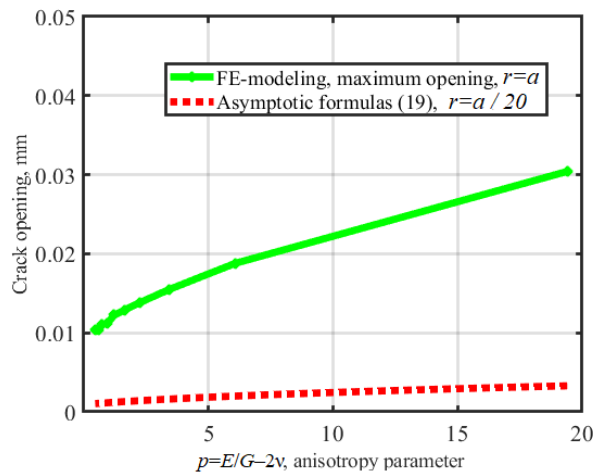


Fig. 6. Dependence of crack opening on anisotropy parameter  $p$ . The maximum disclosure at  $r = a$  (solid line) and opening in the vicinity of the crack tip,  $r = a/20$  (dashed line), are shown

### Conclusions

Analytical expressions for the case of a plane strain state were obtained for stress intensity factors (SIFs) in terms of edge displacements of a rectilinear crack with mixed-mode fracture in an orthotropic material and a material with cubic symmetry. The properties of the influence matrix  $[\mathbf{B}]^{-1}$ , used to find the SIFs, are considered. Just as in the case of a plane stress state (that we discussed earlier in [30]), there is no mode mixing for a material with cubic symmetry (similar to an isotropic material). In contrast to the case of a plane stress state, the coefficients of the influence matrix for an orthotropic material in the case of a plane strain state depend on  $\nu_{13}, \nu_{23}, \nu_{31}, \nu_{32}$ , which in turn relate them to Young's modulus  $E_3$ .

Testing the proposed methods for SIF calculations, we established good agreement with the analytical solution of the problem for a plane with an oblique crack for various crack inclination angles relative to the anisotropy axes of the material in a linear elastic material: isotropic, with cubic symmetry and orthotropic (the error did not exceed 0.75% in all cases). SIF calculation from the stresses in the vicinity of the crack tip gives more accurate results than calculation from the displacements of the crack edges.

Asymptotic formulas were also obtained for crack opening in the cases of isotropic, orthotropic and cubic symmetry material. Crack openings were compared for different classes of materials, depending on their elastic properties, with further confirmation of the results provided by finite element modeling. The dependence of crack opening on the anisotropy parameter  $p$  was obtained for the practically important case of a material with cubic symmetry.

The considered numerical methods for calculating SIFs can be recommended for modeling crack growth and analyzing crack resistance in critical components of gas turbine engines (rotary and static blades) made of single-crystal nickel-based alloys with cubic symmetry of physical and mechanical properties.

## REFERENCES

1. **Semenov A. S., Grishchenko A. I., Kolotnikov M. E., Getsov L. B.**, Finite-element analysis of thermal fatigue of gas turbine blades, Part 1. Material models, fracture criteria, identification, Vestnik UGATU [USATU Bulletin]. 23 (1 (83)) (2019) 70–81 (in Russian).
2. **Getsov L. B., Mikhaylov V. E., Semenov A. S., et al.**, Raschetnoye opredeleniye resursa rabochikh i napravlyayushchikh lopatok GTU. Chast 1. Polikristallicheskiye materialy [Design determination of the work life of operating and guide blades of gas-turbine installations. Part 1. Polycrystalline materials], Gas Turbine Technologies. (7) (2011) 24–30 (in Russian).
3. **Shalin R. E., Svetlov I. L., Kachalov E. B., et al.**, Monokristally nikelovykh zharoprochnykh splavov [Single crystals of nickel heat-resistant alloys], Mashinostroyeniye, Moscow, 1997 (in Russian).
4. **Wilson B. C., Hickman J. A., Fuchs G. E.**, The effect of solution heat treatment on a single-crystal Ni-based superalloy, JOM: J. Minerals, Metals & Mater. Soc. 55 (3) (2003) 35–40.
5. **Getsov L. B.**, Materialy i prochnost detaley gazovykh turbin [Materials and strength of gas turbine parts], in 2 Vols., Vol. 1, Gas Turbine Technologies Publishing, Rybinsk, 2010 (in Russian).
6. **Getsov L. B., Semenov A. S., Ignatovich I. A.**, Thermal fatigue analysis of turbine discs on the base of deformation criterion. Int. J. Fatig. 97 (April) (2017) 88–97.
7. **Wang R., Zhang B., Hu D., et al.**, A critical-plane-based thermomechanical fatigue lifetime prediction model and its application in nickel-based single-crystal turbine blades, Mater. High Temp. 36 (4) (2019) 325–334.
8. **Semenov A. S., Semenov S. G., Getsov L. B.**, Methods of computational determination of growth rates of fatigue, creep, and thermal fatigue cracks in poli- and monocrystalline blades of gas-turbine units, Strength Mater. 47 (2) (2015) 268–290.
9. **Savikovskii A. V., Semenov A. S., Getsov L. B.**, Crystallographic orientation, delay time and mechanical constants influence on thermal fatigue strength of single-crystal nickel superalloys, Mater. Phys. Mech. 44 (1) (2020) 125–136.
10. **Erdogan F.**, Stress intensity factors, J. Appl. Mech. 50 (4b) (1983) 992–1002.
11. **Irwin G. R.**, Analysis of stresses and strains near the end of crack traversing a plate, J. Appl. Mech. 24 (3) (1957) 361–364.
12. **Sih G. C., Paris P. C., Irwin G. R.**, On cracks in rectilinearly anisotropic bodies, Int. J. Fract. Mech. 1 (3) (1965) 189–203.
13. **Ranjan S., Arakere N. K.**, A fracture-mechanics-based methodology for fatigue life prediction of single crystal nickel-based superalloys, J. Eng. Gas Turbine Power. 130 (3) (2008) 032501.
14. **Cho S. B., Lee K. R.**, Determination of stress-intensity factors and boundary element analysis for interface cracks in dissimilar anisotropic materials // Eng. Fract. Mech. 43 (4) (1992) 603–614.
15. **Mauge C., Kachanov M.**, Anisotropic material with interacting arbitrarily oriented cracks stress intensity factors and crack-microcrack interactions, Int. J. Fract. 65 (2) (1994) 115–139.
16. **Tu C.-H., Chen C.-S., Yu T.-T.**, Fracture mechanics analysis of multiple cracks in anisotropic media, Int. J. Numer. Anal. Meth. Geomech. 35 (11) (2011) 1226–1242.
17. **Wang X.-Q., Schubnel A., Fortin J., et al.**, High  $V_p/V_s$  ratio: Saturated cracks or anisotropy effects? Geophys. Res. Lett. 39 (11) (2012) L11307.
18. **Saouma V. E., Ayari M. L., Leavell D. A.**, Mixed mode crack propagation in homogeneous anisotropic solids, Eng. Fract. Mech. 27 (2) (1987) 171–184.
19. **Hakim V., Karma A.**, Crack path prediction in anisotropic brittle materials, Phys. Rev. Lett. 95 (23) (2005) 235501.



20. **Mall S., Murhy J. F., Asce M., Shottafer J. E.**, Criterion for mixed mode fracture in wood, *J. Eng. Mech.* 109 (3) (1983) 680–690.
21. **Ozkan U., Kaya A. C., Loghin A., et al.**, Fracture analysis of cracks in anisotropic materials using 3DFAS and ANSYS, *Proc. ASME Int. Mech. Eng. Congress & Exposition*. Jan., 2006. Chicago, USA (2006) 569–579.
22. **Ozkan U., Nied H. F., Kaya A. C.**, Fracture analysis of anisotropic materials using enriched crack tip elements, *Eng. Fract. Mech.* 77 (7) (2010) 1191–1202.
23. **Song Ch., Tin-Loi F., Gao W.**, A definition and evaluation procedure of generalized stress intensity factors at cracks and multi-material wedges, *Eng. Fract. Mech.* 77 (12) (2010) 2316–2336.
24. **Gao H., Chiu C.**, Slightly curved or kinked cracks in anisotropic elastic solids, *Int. J. Solids Struct.* 29 (8) (1992) 947–972.
25. **Obata M., Nemat-Nasser S., Goto Y.**, Branched cracks in anisotropic elastic solids, *J. Appl. Mech.* 56 (4) (1989) 858–864.
26. **Kardomateas G. A., Li R.**, Thermo-elastic crack branching in general anisotropic media, *Int. J. Solids Struct.* 42 (3–4) (2005) 1091–1109.
27. **Barsoum R. S.**, Cracks in anisotropic materials – an iterative solution of the eigenvalue problem, *Int. J. Fract.* 32 (1) (1986) 59–67.
28. **Mazurowski B., O'Hara P., Gupta P., Duarte C. A.**, A displacement correlation method for stress intensity factor extraction from 3D fractures in anisotropic materials, *Eng. Fract. Mech.* 258 (December) (2021) 108040.
29. **Hoenig A.**, Near-tip behavior of a crack in a plane anisotropic elastic body, *Eng. Fract. Mech.* 16 (3) (1982) 393–403.
30. **Savikovskii A. V., Semenov A. S.**, Calculation of mixed-mode stress intensity factors for orthotropic materials in the plane stress state, *St. Petersburg State Polytechnical University Journal. Physics and Mathematics.* 15 (2) (2022) 102–123 (in Russian).
31. **Lekhnitsky S. G.**, *Teoriya uprugosti anizotropnogo tela [Theory of elasticity of an anisotropic elastic body]*, Nauka, Moscow, 1977 (in Russian).
32. **Voigt W.**, *Lehrbuch der kristallphysik:(mit ausschluss der kristalloptik)*. BG Teubner, Leipzig, Berlin, 1910.
33. **Love A. E. H.**, *Mathematical theory of elasticity*, Cambridge University Press, Cambridge, UK, 1927.
34. **Kachanov M. L.**, *Osnovy mekhaniki razrusheniya [Fundamentals of fracture mechanics]*. Nauka, Moscow, 1974, Pp. 223–226 (in Russian).
35. **Morozov E. N., Nikishkov G. P.**, *Metod konechnykh elementov v mekhanike razrusheniya [Finite element method in fracture mechanics]*, Nauka Publishing, Moscow, 1980 (in Russian).
36. **Judt P. O., Ricoeur A., Linek G.**, Crack path prediction in rolled aluminum plates with fracture toughness orthotropy and experimental validation, *Eng. Fract. Mech.* 138 (April) (2015) 33–48.
37. **Banks-Sills L., Hershkovitz I., Wawrzynek P. A., et al.**, Methods for calculating stress intensity factors in anisotropic materials: Part I.  $z = 0$  is a symmetric plane, *Eng. Fract. Mech.* 72 (15) (2005) 2328–2358.
38. **Khansari N. M., Fakoor M., Berto F.**, Probabilistic micromechanical damage model for mixed-mode I/II fracture investigation of composite materials, *Theor. Appl. Fract. Mech.* 99 (February) (2019) 177–193.
39. **Bathe K. J., Wilson E. L.**, *Numerical methods in finite element analysis*, Prentice-Hall: Englewood Cliffs, New Jersey, USA, 1976.
40. **Gallagher R. H.**, *Finite element analysis: Fundamentals*, Pearson College Div., London, 1975.
41. **Zhao X., Mo Z.-L., Guo Z.-Y., Li J.**, A modified three-dimensional virtual crack closure technique for calculating stress intensity factors with arbitrarily shaped finite element mesh arrangements across the crack front, *Theor. Appl. Fract. Mech.* 109 (October) (2020) 102695.
42. **Fakoor M., Shavsavar S.**, The effect of T-stress on mixed mode I/II fracture of composite materials: Reinforcement isotropic solid model in combination with maximum shear stress theory, *Int. J. Solids Struct.* 229 (15 October) (2021) 111–145.
43. **Semenov A. S.**, *PANTOCRATOR – konechno-elementnyy programmnyy kompleks, oriyentirovanny na resheniye nelineynykh zadach mekhaniki [PANTOCRATOR – finite-element program specialized on the solution of non-linear problems of solid body mechanics]*, In: *Proc. The V-th Int. Conf. “Scientific and engineering problems of reliability and service life of structures and methods of their decision”*, St. Petersburg Polytechnical University Publishing, St. Petersburg (2003) 466–480.

## СПИСОК ЛИТЕРАТУРЫ

1. Семенов А. С., Грищенко А. И., Колотников М. Е., Гецов Л. Б. Конечно-элементный анализ термоциклической прочности лопаток газовых турбин. Ч. 1. Модели материала, критерии разрушения, идентификация параметров // Вестник УГАТУ (Уфимский государственный авиационный технический университет). 2019. Т. 23. № 1 (83). С. 70–81.
2. Гецов Л. Б., Михайлов В. Е., Семенов А. С., Кривоносова В. В., Ножницкий Ю. А., Блинник Б. С., Магеррамова Л. А. Расчетное определение ресурса рабочих и направляющих лопаток ГТУ. Ч. 1. Поликристаллические материалы // Газотурбинные технологии. 2011. № 7. С. 24–30.
3. Шалин Р. Е., Светлов И. Л., Качалов Е. Б., Толораия В. Н., Гаврилин В. С. Монокристаллы никелевых жаропрочных сплавов. М.: Машиностроение, 1997. 336 с.
4. Wilson B. C., Hickman J. A., Fuchs G. E. The effect of solution heat treatment on a single-crystal Ni-based superalloy // JOM: The Journal of the Minerals, Metals & Materials Society. 2003. Vol. 55. No. 3. Pp. 35–40.
5. Гецов Л. Б. Материалы и прочность деталей газовых турбин. В 2 тт. Т. 1. Рыбинск: ИД «Газотурбинные технологии», 2010. 605 с.
6. Getsov L. B., Semenov A. S., Ignatovich I. A. Thermal fatigue analysis of turbine discs on the base of deformation criterion // International Journal of Fatigue. 2017. Vol. 97. April. Pp. 88–97.
7. Wang R., Zhang B., Hu D., Jiang K., Mao J., Jing F. A critical-plane-based thermomechanical fatigue lifetime prediction model and its application in nickel-based single-crystal turbine blades // Materials at High Temperatures. 2019. Vol. 36. No. 4. Pp. 325–334.
8. Семенов А. С., Семенов С. Г., Гецов Л. Б. Методы расчетного определения скорости роста трещин усталости, ползучести и термоусталости в поли- и монокристаллических лопатках ГТУ // Проблемы прочности. 2015. № 2. С. 61–87.
9. Savikovskii A. V., Semenov A. S., Getsov L. B. Crystallographic orientation, delay time and mechanical constants influence on thermal fatigue strength of single-crystal nickel superalloys // Materials Physics and Mechanics. 2020. Vol. 44. No. 1. Pp. 125–136.
10. Erdogan F. Stress intensity factors // Journal of Applied Mechanics. 1983. Vol. 50. No. 4b. Pp. 992–1002.
11. Irwin G. R. Analysis of stresses and strains near the end of crack traversing a plate // Journal of Applied Mechanics. 1957. Vol. 24. No. 3. Pp. 361–364.
12. Sih G. C., Paris P. C., Irwin G. R. On cracks in rectilinearly anisotropic bodies // International Journal of Fracture Mechanics. 1965. Vol. 1. No. 3. Pp. 189–203.
13. Ranjan S., Arakere N. K. A fracture-mechanics-based methodology for fatigue life prediction of single crystal nickel-based superalloys // Journal of Engineering for Gas Turbines and Power. 2008. Vol. 130. No. 3. P. 032501.
14. Cho S. B., Lee K. R. Determination of stress-intensity factors and boundary element analysis for interface cracks in dissimilar anisotropic materials // Engineering Fracture Mechanics. 1992. Vol. 43. No. 4. Pp. 603 – 614.
15. Mauge C., Kachanov M. Anisotropic material with interacting arbitrarily oriented cracks stress intensity factors and crack-microcrack interactions // International Journal of Fracture. 1994. Vol. 65. No. 2. Pp. 115–139.
16. Tu C.-H., Chen C.-S., Yu T.-T. Fracture mechanics analysis of multiple cracks in anisotropic media // International Journal for Numerical and Analytical Methods in Geomechanics. 2011. Vol. 35. No. 11. Pp. 1226–1242.
17. Wang X.-Q., Schubnel A., Fortin J., David E.C., Gueguen Y., Ge H.-K. High  $V_p/V_s$  ratio: Saturated cracks or anisotropy effects? // Geophysical Research Letters. 2012. Vol. 39. No. 11. P. L11307.
18. Saouma V. E., Ayari M. L., Leavell D. A. Mixed mode crack propagation in homogeneous anisotropic solids // Engineering Fracture Mechanics. 1987. Vol. 27. No. 2. Pp. 171–184.
19. Hakim V., Karma A. Crack path prediction in anisotropic brittle materials // Physical Review Letters. 2005. Vol. 95. No. 23. P. 235501.
20. Mall S., Murhy J. F., Asce M., Shottafer J. E. Criterion for mixed mode fracture in wood // Journal of Engineering Mechanics. 1983. Vol. 109. No. 3. Pp. 680–690.





21. **Ozkan U., Kaya A. C., Loghin A., Ayhan A. O., Nied H. F.** Fracture analysis of cracks in anisotropic materials using 3DFAS and ANSYS // Proceedings of ASME International Mechanical Engineering Congress and Exposition. January, 2006. Chicago, USA. Pp. 569–579.
22. **Ozkan U., Nied H. F., Kaya A. C.** Fracture analysis of anisotropic materials using enriched crack tip elements // Engineering Fracture Mechanics. 2010. Vol. 77. No. 7. Pp. 1191–1202.
23. **Song Ch., Tin-Loi F., Gao W.** A definition and evaluation procedure of generalized stress intensity factors at cracks and multi-material wedges // Engineering Fracture Mechanics. 2010. Vol. 77. No. 12. Pp. 2316–2336.
24. **Gao H., Chiu C.** Slightly curved or kinked cracks in anisotropic elastic solids // International Journal of Solids and Structures. 1992. Vol. 29. No. 8. Pp. 947–972.
25. **Obata M., Nemat-Nasser S., Goto Y.** Branched cracks in anisotropic elastic solids // Journal of Applied Mechanics. 1989. Vol. 56. No. 4. Pp. 858–864.
26. **Kardomateas G. A., Li R.** Thermo-elastic crack branching in general anisotropic media // International Journal of Solids and Structures. 2005. Vol. 42. No. 3–4. Pp. 1091–1109.
27. **Barsoum R. S.** Cracks in anisotropic materials – an iterative solution of the eigenvalue problem // International Journal of Fracture. 1986. Vol. 32. No. 1. Pp. 59–67.
28. **Mazurowski B., O’Hara P., Gupta P., Duarte C. A.** A displacement correlation method for stress intensity factor extraction from 3D fractures in anisotropic materials // Engineering Fracture Mechanics. 2021. Vol. 258. December. P. 108040.
29. **Hoening A.** Near-tip behavior of a crack in a plane anisotropic elastic body // Engineering Fracture Mechanics. 1982. Vol. 16. No. 3. Pp. 393–403.
30. **Савиковский А. В., Семенов А. С.** Вычисление коэффициентов интенсивности напряжений в ортотропных материалах при смешанной моде разрушения в плоском напряженном состоянии // Научно-технические ведомости СПбГПУ. Физико-математические науки. 2022. Т. 15. № 2. С. 102–123.
31. **Лехницкий С. Г.** Теория упругости анизотропного тела. М.: Наука, 1977. 416 с.
32. **Voigt W.** Lehrbuch der kristallphysik:(mit ausschluss der kristalloptik). Leipzig, Berlin: BG Teubner, 1910. s.
33. **Ляв А.** Математическая теория упругости. Пер. с англ. Ленинград: Объединенное научно-техническое издательство (ОНТИ), 1935. 672 с.
34. **Качанов Л. М.** Основы механики разрушения. М.: Наука, 1974. С. 223–226.
35. **Морозов Е. Н., Никишков Г. П.** Метод конечных элементов в механике разрушения. М.: Наука, 1980. 256 с.
36. **Judt P. O., Ricoeur A., Linek G.** Crack path prediction in rolled aluminum plates with fracture toughness orthotropy and experimental validation // Engineering Fracture Mechanics. 2015. Vol. 138. April. Pp. 33–48.
37. **Banks-Sills L., Hershkovitz I., Wawrzynek P. A., Eliasi R., Ingraffea A. R.** Methods for calculating stress intensity factors in anisotropic materials: Part I.  $z = 0$  is a symmetric plane // Engineering Fracture Mechanics. 2005. Vol. 72. No. 15. Pp. 2328–2358.
38. **Khansari N. M., Fakoor M., Berto F.** Probabilistic micromechanical damage model for mixed-mode I/II fracture investigation of composite materials // Theoretical and Applied Fracture Mechanics. 2019. Vol. 99. February. Pp. 177–193.
39. **Bathe K. J., Wilson E. L.** Numerical methods in finite element analysis. . New Jersey, USA: Prentice-Hall: Englewood Cliffs, 1976. 528 p.
40. **Gallagher R. H.** Finite element analysis: Fundamentals. London: Pearson College Div., 1975. 420 p.
41. **Zhao X., Mo Z.-L., Guo Z.-Y., Li J.** A modified three-dimensional virtual crack closure technique for calculating stress intensity factors with arbitrarily shaped finite element mesh arrangements across the crack front // Theoretical and Applied Fracture Mechanics. 2020. Vol. 109. October. P. 102695.
42. **Fakoor M., Shavsavar S.** The effect of T-stress on mixed mode I/II fracture of composite materials: Reinforcement isotropic solid model in combination with maximum shear stress theory // International Journal of Solids and Structures. 2021. Vol. 229. 15 October. Pp. 111–145.
43. **Семенов А. С.** PANTOCRATOR – конечно-элементный программный комплекс, ориентированный на решение нелинейных задач механики // Труды V-ой Международной конференции «Научно-технические проблемы прогнозирования надежности и долговечности конструкций». СПб.: Изд-во СПбГПУ, 2003. С. 466–480.

## THE AUTHORS

**SAVIKOVSKII Artem V.**

*Peter the Great St. Petersburg Polytechnic University*  
29 Politechnicheskaya St., St. Petersburg, 195251, Russia  
savikovskii.artem@yandex.ru  
ORCID: 0000-0003-1710-1943

**SEMENOV Artem S.**

*Peter the Great St. Petersburg Polytechnic University*  
29 Politechnicheskaya St., St. Petersburg, 195251, Russia  
Semenov.Artem@googlemail.com  
ORCID: 0000-0002-8225-3487

**СВЕДЕНИЯ ОБ АВТОРАХ**

**САВИКОВСКИЙ Артем Викторович** – аспирант кафедры «Механика и процессы управления» Санкт-Петербургского политехнического университета Петра Великого.

195251, Россия, г. Санкт-Петербург, Политехническая ул., 29

savikovskij.av@edu.spbstu.ru

ORCID: 0000-0003-1710-1943

**СЕМЕНОВ Артем Семенович** – доктор физико-математических наук, заведующий кафедрой сопротивления материалов Санкт-Петербургского политехнического университета Петра Великого.

195251, Россия, г. Санкт-Петербург, Политехническая ул., 29

Semenov.Artem@googlemail.com

ORCID: 0000-0002-8225-3487

*Статья поступила в редакцию 29.09.2022. Одобрена после рецензирования 14.05.2023. Принята 14.05.2023.*

*Received 29.09.2022. Approved after reviewing 14.05.2023. Accepted 14.05.2023.*